A New Analytical and Experimental Approach To Rubber Thermodynamics

D. J. Macon† and R. J. Farris*

Polymer Science and Engineering Department, University of Massachusetts, Amherst, Massachusetts 01003

Received April 28, 1998; Revised Manuscript Received March 16, 1999

ABSTRACT: The statistical theory of rubber elasticity is thermodynamically reanalyzed using a proper temperature reference state, which proves that the energetic contribution to the stress, resulting from temperature changes, is equal to zero. This is in contrast to the traditional analysis that yields a nonzero energetic term even though the theory is derived by assuming purely entropic contributions. Using a proper temperature reference state, a nonlinear thermoelastic constitutive equation is obtained from a strain energy function and empirical observations about the stress-temperature behavior of elastomeric materials. This relationship is used to model the thermoelastic behavior of cross-linked natural rubber that had the thermoelastic response measured using vibrational holographic interferometry. Holographic interferometry allows resolution of the true principal stresses of a thin film in uniaxial or biaxial extension. Thermoelastic data for natural rubber in uniaxial and biaxial extension have been successfully modeled using the constitutive approach presented.

Introduction

A number of theories have been developed to describe the stress−deformation process for rubbery materials. Rivlin was among the first to use a continuum phenomenological expression to describe large deformations of elastomers at constant temperature.[1] Another popular theory is the statistical thermodynamic approach expounded upon by Flory.[2] This theory assumes affine deformation of cross-linked junctions and no internal energy change with isothermal deformation. When deformation processes that involve a change in temperature are analyzed, the modeling situation becomes more complicated. In the statistical theory, a single modulus is prescribed to account for these changes in stress with temperature. This single parameter is set directly proportional to the absolute temperature and is generally assumed to contain all of the temperature dependence. Lu and Pister used a different approach to account for thermal effects by describing the process as a combination of free thermal expansion and isothermal mechanical deformation.[3] Recently, more effort has been exerted to describe the thermoelastic deformation process using this type of approach.[4,5]

Considerable effort has been devoted to using the statistical theory to establish the entropic and energetic contributions resulting from thermomechanical deformation, and several reviews on these results have been written.[6−21] By using a thermodynamic approach, several researchers have used this theory to calculate a nonzero term for the internal energy contribution to the stress resulting from isothermal deformation.[6,10,13−16,18,19] This result violates one of the basic assumptions of the statistical theory. One purpose of this paper to establish that this nonzero term is merely an artifact of an improper temperature reference state. A proper reference state needs to be chosen for any parameter (e.g., extension ratios, area, volume, etc.) that depends on the initial dimensions. It is especially essential to choose a proper reference temperature for the moduli, since they too depend on the initial dimensions.

Several methods for measuring the thermoelastic behavior of rubbery materials have been devised. These methods typically uniaxially stretch a piece of rubber to some fixed deformation and measure the force or engineering stress as a function of temperature.[9,10,12,14,16] Some researchers have also measured the isothermal and thermal behavior of rubber samples under biaxial extension, but very little attention has been devoted to the thermoelastic behavior of elastomers under anisotropic biaxial extension.[25,32−35] Problems with these measurement techniques vary but can include electronic drift in equipment during the long times required to achieve thermal and stress equilibrium and changes in the dimensions of the testing hardware with temperature.

The proposed method for correcting these measurement problems is to employ time-average vibrational holographic interferometry. This technique allows resolution of one or more of the principal stresses of a thin film in either uniaxial extension or isotropic and anisotropic biaxial extension to a degree of high accuracy. Holographic interferometry allows a variety of other measurements to be made, including directly measuring the total state of stress, the through the thickness diffusion coefficients of a thin film, and the linear elastic constants.[36−40]

A Proper Reference State

In any thermomechanical deformation, the deformation process needs to be properly mapped as it undergoes a change in dimensions resulting from either mechanical or thermal processes. A proper thermoelastic treatment should account for the changes in configuration resulting from thermal expansion. Figure 1 shows an elastic body that is deformed by the combined application of heat and an applied load. If the path A → B is followed, the temperature on an unconstrained stress-free body changes from the initial temperature,

* To whom correspondence should be addressed.
† Present address: Thiokol Corporation, PO Box 707, M/S 243, Brigham City, UT 84302-0707.

10.1021/ma9806763 CCC: $18.00
Published on Web 07/01/1999

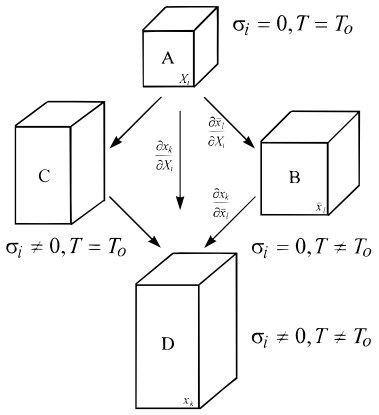

Figure 1. Physical description of thermomechanical deformation.

T_o, to temperature, T, resulting in unconstrained thermal expansion. Afterward if some load is applied, the body isothermally deforms to a new configuration as shown by path B → D. Alternatively, the same process may be described by path A → C → D. First, stress is applied to the body, which isothermally deforms to a new configuration. Second, heat is added to the stressed body causing constrained thermal expansion of the body. Either path A → B → D or path A → C → D properly accounts for both the mechanical and thermal histories of the body, but in this paper only the former path will be considered. More details about this type of approach are described by Lu and Pister.[3]

To describe the two-step deformation processes, a Lagrangian strain measure is used, which requires referencing the strain to a fixed-stress, free-reference state.[22,23] Also, indicial notation is used and summations are implied except where noted. The full strain history for both thermal and mechanical deformations (path A → B → D) is given by

$$dx_k = \frac{\partial x_k}{\partial X_i} dX_i \tag{1}$$

or by the chain rule as

$$dx_k = \frac{\partial x_k \partial \bar{x}_l}{\partial \bar{x}_l \partial X_i} dX_i \tag{2}$$

where X_i are material coordinates of some particle in an elastic body under stress-free conditions at reference temperature, T_o, x_k are the particle positions after isothermal deformation, and $\bar{x}_l$ are the spatial coordinates of the particle after unconstrained thermal expansion from reference temperature, T_o, to current temperature, T.

The deformation gradient tensor defined in eq 1 can be used to describe the work, W, done by deforming the material. The dependence of W on $\partial x_k/\partial X_i$ is obtained through the symmetric right Cauche−Green strain tensor, $\mathbf{C}_{ij}$, defined as

$$\mathbf{C}_{ij} = \frac{\partial x_k \partial x_k}{\partial X_i \partial X_j} \tag{3}$$

with the principal invariants of $\mathbf{C}_{ij}$

$$I_1 = \text{tr } \mathbf{C}_{ij}$$

$$I_2 = \frac{1}{2}[(\text{tr } \mathbf{C}_{ij})^2 - \text{tr } \mathbf{C}_{ij}^2]$$

$$I_3 = \det \mathbf{C}_{ij}$$

It has been observed that the length of an unstressed isotropic body increases with temperature over a fairly broad region of temperature as

$$\frac{\partial \bar{x}_l}{\partial X_i} = \delta_{li} e^{\alpha(T-T_o)} \tag{4}$$

where δ_{li} is the Kronecker δ and α is the linear stress-free coefficient of thermal expansion.[26] Substituting this expression into the strain tensor and making use of the chain rule yields

$$\mathbf{C}_{ij} = \frac{\partial x_k}{\partial \bar{x}_l}\frac{\partial x_k}{\partial \bar{x}_m} e^{2\alpha(T-T_o)} \delta_{li}\delta_{mj} = \frac{\partial x_k}{\partial \bar{x}_i}\frac{\partial x_k}{\partial \bar{x}_j} e^{2\alpha(T-T_o)} = \tilde{C}_{ij} e^{2\alpha(T-T_o)} \tag{5}$$

where $\tilde{C}_{ij}$ is the strain matrix representing isothermal deformation. This large strain expression has the shear strains depending upon the coefficient of thermal expansion. Constitutive equation are often expressed in terms of the Lagrangian strain tensor (large strain), but the shear strains are written as having no dependence upon the temperature.

In relating the deformation gradients to the more familiar forms found in the literature, we introduce the following notation

$$\frac{\partial x_i}{\partial X_i} = \lambda_i(T_o), \quad \frac{\partial x_i}{\partial \bar{x}_i}\bar{\lambda}_i(T) \quad \text{(no sum)} \tag{6}$$

where $\lambda_i(T_o)$ are the extension ratios referenced to temperature, T_o, and represent the stretch ratios resulting from both thermal and mechanical deformation; $\bar{\lambda}_i(T)$ are the extension ratios referenced to temperature, T, and represent isothermal deformation.

These $\bar{\lambda}_i(T)$ are the same λ_i's used in the statistical and continuum approaches to rubber elasticity. The extension ratios are related as $\lambda_i(T_o) = \bar{\lambda}_i(T)e^{\alpha(T-T_o)}$. The notation (T_o) is taken throughout to designate that a particular parameter is referenced to reference temperature, T_o, and (T) denotes that a parameter is referenced to temperature, T. Likewise, (T,T) and (T,T_o) will be used to show that a parameter is a function of temperature and is referenced to temperature T or T_o, respectively.

The strain energy, an invariant, becomes a function of the strain invariants and is typically written as a power series

$$\bar{W}(T,T) = \sum_{ijk=0}^{\infty} \bar{C}_{ijk}(T,T)(\bar{I}_1(T) - 3)^i(\bar{I}_2(T) - 3)^j(\bar{I}_3(T) - 1)^k \bar{V}_o(T) \tag{7}$$

where $\bar{W}(T,T)$ is the strain energy, $\bar{V}_o(T)$ is the undeformed volume, and $\bar{C}_{ijk}(T,T)$ are the Rivlin elastic constants with $\bar{C}_{000}(T,T)$ being equal to zero.

If the reference state for the strain energy is changed from T to T_o, the strain energy may be rewritten as

$$W(T,T_o) = \sum_{ijk=0}^{\infty}\left[\bar{C}_{ijk}(T,T)(I_1(T_o)e^{-2\alpha\Delta T} - 3)^i(I_2(T_o)e^{-4\alpha\Delta T} - 3)^j (I_3(T_o)e^{-6\alpha\Delta T} - 1)^k\right]V_o(T_o)e^{3\alpha\Delta T} \quad (8)$$

where $\Delta T = T - T_o$.

The Rivlin elastic constants in eq 8 have been written so that they are referenced to temperature, T. To transform the constants to reference temperature, T_o, it is noted that the strain energy is invariant regardless of reference state, (i.e., $\bar{W}(T,T) \equiv W(T,T_o)$). This demands that $\bar{C}C_{ijk}(T,T) = \mathbf{C}_{ijk}(T,T_o)e^{n\alpha\Delta T}$ where $n = -3 + 2i + 4j + 6k$, (e.g., $\bar{C}_{010}(T,T) = C_{010}(T,T_o)e^{\alpha\Delta T}$, $\bar{C}_{111}(T,T) = C_{111}(T,T_o)e^{9\alpha\Delta T}$). It is important to note that the material constants are referenced differently, because they also have a dependence upon the initial dimensions. In the statistical theory of rubber elasticity, a single term from the strain energy expression given in eq 7 is used.

Expressions for the Strain Energy

The possible terms of the strain energy are limitless with the exception that the resulting stress must reduce to linear elasticity in the limit of vanishing strain (i.e., the constitutive equation contains two material constants).[26] Treloar applied the kinetic theory of rubber elasticity to an assumed incompressible cube of vulcanized rubber yielding a strain energy expression of the form[27]

$$\bar{W}(T,T) = \bar{C}_{100}(T,T)(\bar{I}_1(T) - 3)\bar{V}_o(T) \quad (9)$$

This expression is called the neo-Hookean form and is mathematically equivalent to the Gaussian free energy of deformation, but will not reduce to general linear elasticity. Mooney proposed on purely phenomenological grounds[28]

$$\bar{W}(T,T) = [\bar{C}_{100}(T,T)(\bar{I}_1(T) - 3) + \bar{C}_{010}(T,T)(\bar{I}_2(T) - 3)]\bar{V}_o(T) \quad (10)$$

This expression is known as the Mooney−Rivlin form of the strain energy. Blatz showed that the two Rivlin constants, (i.e., C_1 and C_2) combine in the limits of small temperature changes and finite deformation to form a single shear modulus.[29]

To account for thermal effects, the neo-Hookean strain energy assigns the entire temperature dependence of the equation to the material constant as

$$\bar{C}_{100}(T,T) = \frac{1}{2}N_oRT \approx \frac{1}{2}\bar{G}_o(T,T) \quad (11)$$

where N_o is the number of moles of network chains per unit volume of the undeformed sample, R is the ideal gas constant, T is the current temperature, and $\bar{G}_o(T,T)$ is the shear modulus.[30] Parameters that depend on the undeformed dimensions (e.g., λ, V_o, etc.) are not corrected for changes in configuration resulting from temperature fluctuations. This treatment is the same as mathematically following path A → D in Figure 1. Also, $\bar{C}_{100}(T,T)$ is not referenced to a particular temperature, which makes it difficult to assign the constant an experimentally measured value. When properly referenced, the material constant is written as $C_{100}(T,T_o) = \bar{C}_{100}(T,T)e^{\alpha\Delta T}$.

If the dependence of $\bar{W}(T,T)$ on $\bar{\lambda}_i(T)$ or $W(T,T_o)$ on $\lambda_i(T_o)$ is known, the nominal or engineering stress, σ_i^o, may be derived from

$$\sigma_i^o(T,T_o)V_o(T_o) = \frac{\partial W(T,T_o)}{\partial\lambda_i(T_o)} \text{ or } \bar{\sigma}_i^o(T,T)\bar{V}_o(T) = \frac{\partial\bar{W}(T,T)}{\partial\bar{\lambda}_i(T)} \quad (12)$$

The engineering stress as a function of temperature referenced to temperature, T_o, resulting from uniaxial deformation is

$$\sigma_1^o(T,T_o) = 2C_{100}(T,T_o)\left(\lambda_1(T_o) - \frac{J(T,T_o)}{\lambda_1^2(T_o)}\right) \quad (13)$$

where $J(T,T_o)$ is the dilatation and is defined as $J(T,T_o) = \lambda_1(T_o)\lambda_2(T_o)\lambda_3(T_o) = \bar{V}(T)/V_o(T_o)$, and $\bar{V}(T)$ is the deformed volume. Alternatively, the nominal stress as a function of temperature referenced to temperature, T, is

$$\bar{\sigma}_1^o(T,T) = 2\bar{C}_{100}(T,T)\left(\bar{\lambda}_1(T) - \frac{\bar{J}(T,T)}{\bar{\lambda}_1^2(T)}\right) \quad (14)$$

These two expressions differ from each other in that eq 13 has parameters that only depend on the initial dimensions referenced to a particular temperature. However, in eq 14, the initial dimensions change as the temperature is changed, and this is the usual method that is used in the reference literature. The differences between the expressions are particularly important when they are thermodynamically analyzed.

Energetic Contribution to the Stress

Several investigators have examined how the energetic contribution to the stress resulting from isothermal deformation of a rubbery material may be established. In the vast majority of these efforts, the authors start with the statistical theory of rubber elasticity, which is based on the assumption of ideal rubber behavior (i.e., pure entropy). Yet when the same relations are manipulated according to thermodynamics, an energetic term is revealed.[6−19]

The Maxwell relations can be manipulated to yield an expression for the relative energy contribution, f_e/f, resulting from isothermal deformation as

$$\frac{f_e}{f} = 1 - T\left(\frac{\partial(\ln f)}{\partial T}\right)_{\bar{L}(T),\bar{V}(T)} \quad (15)$$

where $f_e = (\partial U/\partial\bar{L}(T))_{T,\bar{V}(T)}$, U is the internal energy, $\bar{L}(T)$ is the deformed length of the sample, and f is the force.[30]

One can rewrite eqs 13 and 14 in terms of the force as

$$f = \bar{\sigma}_1^o(T,T)\bar{A}_o(T) = 2\bar{C}_{100}(T,T)\bar{A}_o(T)\left(\bar{\lambda}_1(T) - \frac{\bar{J}(T,T)}{\bar{\lambda}_1^2(T)}\right) \quad (16)$$

$$f = \sigma_1^o(T,T_o)A_o(T_o) = 2C_{100}(T,T_o)A_o(T_o)\left(\lambda_1(T_o) - \frac{J(T,T_o)}{\lambda_1^2(T_o)}\right) \quad (17)$$

where $\bar{A}_o(T)$ and $A_o(T_o)$ are the undeformed cross-sectional areas. The equations listed above are two separate relations and are usually not written explicitly because the equations are typically not referenced to a particular temperature. Calculating f_e/f for the two expressions above and using $C_{100}(T,T_o) = \bar{C}_{100}(T,T)e^{\alpha\Delta T}$ gives

$$\frac{f_e}{f} = 1 - \alpha T - T\left(\frac{\partial(\ln \bar{C}_{100}(T,T))}{\partial T}\right)_{\bar{L}(T),\bar{V}(T)} \quad (18)$$

and

$$\frac{f_e}{f} = 1 - T\left(\frac{\partial(\ln C_{100}(T,T_o))}{\partial T}\right)_{\bar{L}(T),\bar{V}(T)} \quad (19)$$

The αT in eq 18 is a result of the reference state and is an artifact. However, in eq 19, the initial dimensions (e.g., V_o, l_o, etc.) are not functions of temperature, because these dimensions are referenced to temperature, T_o. Equation 18 can still be used to support the rubber elasticity supposition that f_e/f, if a proper reference point for the material constant is used. As noted earlier $\bar{C}_{100}(T,T) = C_{100}(T,T_o)e^{-\alpha\Delta T}$, and if it is assumed that the material is an ideal rubber, the material constant can be assigned a value of

$$C_{100}(T,T_o) = \frac{N_o R T}{2} \quad (20)$$

Substituting these expressions into eqs 18 and 19, yields for both equations

$$\frac{f_e}{f} = 0 \quad (21)$$

This is in agreement with the definition of an ideal rubber. Shen and Blatz reached a similar conclusion in which they assigned the shear modulus the form

$$G(T,T_o) = G(T_o,T_o)(T/T_o)e^{-m\beta\Delta T/3} \quad (22)$$

where m is a constant; $G(T_o,T_o)$ is the shear modulus as a function of temperature, T_o, and is referenced to temperature, T_o, and β is the volumetric coefficient of thermal expansion. Using this definition, they conclude

$$\frac{f_e}{f} = (m - 1)(\beta T/3) \quad (23)$$

which is the same as our result when $m = 1$. However, they did not recognize that moduli depend on a reference temperature and that $m = 1$ for all materials when one references values to the proper temperature.

Vibrational Holographic Interferometry

Vibrational holographic interferometry is an experimental approach that allows thermoelastic measurements to be conducted. For a membrane in an anisotropic state of biaxial stress, the Cauchy or true stress tensor, σ_{ij}, may be written as

$$\sigma_{ij} = \begin{bmatrix} \sigma_{11} & \sigma_{12} & 0 \\ \sigma_{12} & \sigma_{22} & 0 \\ 0 & 0 & 0 \end{bmatrix} \quad (24)$$

It is assumed that the in-plane true stress for such a system has a dominating influence upon its natural frequencies.[41] The governing equation for any membrane in a state of anisotropic biaxial stress under vacuum is

$$\sigma_{11}\frac{\partial^2 w}{\partial x_1^2} + 2\sigma_{12}\frac{\partial^2 w}{\partial x_1 \partial x_2} + \sigma_{22}\frac{\partial^2 w}{\partial x_2^2} = \bar{\rho}(T)\frac{\partial^2 w}{\partial t^2} \quad (25)$$

where w is the out-of-plane displacement, t is the time, $\bar{\rho}(T)$ is the deformed density of the membrane, and x_1 and x_2 are coordinate directions.[42] Certain assumptions are made when using this equation:[43]

1. The in-plane stress is assumed to be homogeneous.
2. The membrane is of uniform thickness.
3. The out-of-plane displacement is sufficiently small such that the state of strain and hence stress is not affected by vibration.
4. The thickness and modulus of the membrane are small enough to neglect the bending stiffness.

The governing equation allows determination of all three terms of the stress tensor, or the two principal stresses and the angle of orientation of the principal axes.[38] If a square membrane is oriented with its edges aligned along the principal directions, the shear stress terms, σ_{12}, disappear and the governing equation reduces to

$$\sigma_1\frac{\partial^2 w}{\partial x_1^2} + \sigma_2\frac{\partial^2 w}{\partial x_2^2} = \bar{\rho}(T)\frac{\partial^2 w}{\partial t^2} \quad (26)$$

where σ_1 and σ_2 are the two principal true stresses. The edges can be assumed to be fixed, giving no out-of-plane displacement at the edges

$$w = 0 \quad \text{at} \quad x_1 = 0, \quad x_2 = 0, \quad x_1 = L, \quad x_2 = L$$

where L is the length of the square membrane.[37] Using these boundary conditions, the solution to eq 26 becomes

$$w(x_1,x_2,t) = K \sin\left(\frac{m\pi}{L}x_1\right)\sin\left(\frac{n\pi}{L}x_2\right)\sin(\omega_{mn}t) \quad (27)$$

where ω_{mn} are the resonant angular frequencies. At other frequencies, it is assumed that there is no out-of-plane displacement, (i.e., $w(x_1,x_2,t) = 0$). Substituting eq 27 into eq 26 and solving the differential equation yields

$$\sigma_1 m^2 + \sigma_2 n^2 = 4\bar{\rho}(T)(\upsilon_{mn})^2 L^2 \quad (28)$$

where $\upsilon_{mn} = {}^1/_2\pi\ \omega_{mn}$ are the resonant frequencies of the sample and can be experimentally determined when the sample is vibrating at its natural frequencies and m and n are integer mode numbers used to describe the many modes of vibration that can be observed.

In eq 28, the deformed density is difficult to measure, but can be related to the undeformed density and the dilatation as a function of temperature referenced to temperature, T_o, by the use of

$$\bar{\rho}(T) = \frac{\rho(T_o)}{J(T,T_o)} \quad (29)$$

where $\rho(T_o)$ is the undeformed density. Substituting this definition back into eq 28 yields

$$\sigma_1 J(T,T_o)m^2 + \sigma_2 J(T,T_o)n^2 = 4\rho(T_o)(\upsilon_{mn})^2 L^2 \quad (30)$$

To directly measure the principal stresses, the resonant frequencies of the membrane are measured as a function of temperature (ranging from −50 to +400 °C), and the vibrational modes are visualized in real time. Several modes of vibration can be detected, (e.g., $(m,n) = (1,1), (1,2), (2,1), (2,2), \ldots$). Once the resonant frequencies have been established, the principal stresses can be very accurately determined. For the case of uniaxial extension, the first principal stress can be established using the 1-dimensional equivalent of eq 30, or for the case of anisotropic biaxial extension, the first two principal stresses can be found using a linear regression method.

Holographic interferometry has several advantages over traditional methods used to make thermoelastic measurements. Accurate measurements require equilibrium conditions which are difficult to obtain because of electronic drift of load cells and their instrumentation. Holographic interferometry eliminates this error because the sample is constantly constrained and the biaxial stresses in the membrane are directly determined using no load cells. Another problem with traditional measurement techniques is the change in the length of the sample gripping hardware with temperature. By constraint of the sample with a washer with a low linear coefficient of thermal expansion, hardware thermal effects can essentially be eliminated.

Analysis of Anisotropic Biaxial Stress Data

Measuring the two principal stresses of a rubbery material in a state of anisotropic biaxial extension allows simplification of the thermoelastic analysis. A variety of terms can be been retained from eq 8 to describe the stress−strain behavior of an elastomeric material under both isothermal and nonisothermal conditions. For this discussion, we are interested in expressions that reduce to linear thermoelasticity in the limit of small strains and small temperature changes.[26] It has been shown by Lyon and Farris that volume changes determine the entropic contribution and influence the internal energy component of deformation for classical linear thermoelastic solids.[31] With this in mind, it seems logical that any phenomenological expression derived from the strain energy density should reduce to a deviatoric and a spherical component.

The first three terms in the Rivlin expansion of the strain energy density will not reduce to linear thermoelasticity. Three terms of higher order are necessary. For the simplest case, two of the terms can be first order with the remaining term being second order or higher. The following equation illustrates a possible expansion of the strain energy density that reduces to thermoelasticity.

$$W(T,T_o) = [C_{100}(T,T_o)(I_1(T_o) - 3e^{2\alpha\Delta T}) + C_{001}(T,T_o)(I_3(T_o) - 3e^{6\alpha\Delta T}) + C_{002}(T,T_o)(I_3(T_o) - 3e^{6\alpha\Delta T})^2]V_o(T_o) \quad (31)$$

The first two terms of this equation combine into a single term in the limit of small strains and small temperature changes and represent the deviatoric component. The final term reduces to the spherical component in the same limits.

The principal true stress can be derived using

$$V_o(T_o)\sigma_i = \frac{\lambda_i(T_o)}{J(T,T_o)}\left(\frac{\partial W(T,T_o)}{\partial \lambda_i(T_o)}\right) \quad (32)$$

The two principal true stresses for biaxial extension become

$$\sigma_1 = \left[2C_{100}(T,T_o)\left(\frac{\lambda_1^2(T_o)}{J(T,T_o)} - \frac{J(T,T_o)}{\lambda_1^2(T_o)\,\lambda_2^2(T_o)}\right) + 2C_{001}(T,T_o)J(T,T_o) + 4C_{002}(T,T_o)J(T,T_o)(J^2(T,T_o) - e^{6\alpha\Delta T})^2\right] \quad (33)$$

$$\sigma_2 = \left[2C_{100}(T,T_o)\left(\frac{\lambda_2^2(T_o)}{J(T,T_o)} - \frac{J(T,T_o)}{\lambda_1^2(T_o)\,\lambda_2^2(T_o)}\right) + 2C_{001}(T,T_o)J(T,T_o) + 4C_{002}(T,T_o)J(T,T_o)(J^2(T,T_o) - e^{6\alpha\Delta T})^2\right] \quad (34)$$

Subtracting these two equations from each other and rearranging yields

$$\Delta\sigma J(T,T_o) = 2C_{100}(T,T_o)(\lambda_1^2(T_o) - \lambda_2^2(T_o)) \quad (35)$$

where $\Delta\sigma = \sigma_1 - \sigma_2$.

This form of the first normal stress difference greatly simplifies the thermodynamic analysis. If the strain energy density function is defined differently from eq 31, the resulting first normal stress difference may result in a form different from eq 35. However, for this paper, the analysis will be limited to this equation.

It is interesting to note that when eq 35 is thermodynamically analyzed, the internal energy contribution to the stress is equal to zero. From Appendix 1, the relative energy contribution, $\Delta\sigma'_E/\Delta\sigma'$, is

$$\frac{\Delta\sigma'_E}{\Delta\sigma'} = 1 - T\frac{1}{\Delta\sigma' J(T,T_o)}\left[\left(\frac{\partial\Delta\sigma' J(T,T_o)}{\partial T}\right)_{P,\lambda_1(T_o),\lambda_2(T_o)} + \left(\frac{\partial P}{\partial T}\right)_{J(T,T_o),\lambda_1(T_o),\lambda_2(T_o)}\left(\frac{\partial\Delta\sigma' J(T,T_o)}{\partial P}\right)_{T,\lambda_1(T_o),\lambda_2(T_o)}\right] \quad (36)$$

If the material is assumed to behave as an ideal rubber (i.e., $C_{100}(T,T_o) = {}^1/_2 N_o RT$), eq 35 becomes

$$\Delta\sigma J(T,T_o) = N_o RT(\lambda_1^2(T_o) - \lambda_2^2(T_o)) \quad (37)$$

If this definition is used the partial derivative, $(\partial\Delta\sigma' J(T,T_o)/\partial P)_{T,\lambda_1(T_o),\lambda_2(T_o)}$, is equal to zero, and eq 36 becomes

$$\frac{\Delta\sigma'_E}{\Delta\sigma'} = 0 \quad (38)$$

This is consistent with the definition of an ideal rubber, and if true, a plot of $\Delta\sigma J(T,T_o)$ vs absolute temperature should intersect at the origin.

Experimental Procedure

Pale crepe natural rubber is cured in a hot press at 140 °C for 40 min using 1.5 phr dicumyl peroxide as a cross-linking agent. The sample is then post-cured at 70 °C for 12 h under vacuum. Afterward, a wire screen of 100 lines-per-inch is superimposed over the surface, and gold is sputter coated over the screen, leaving a mesh pattern on the film. For uniaxial measurements, a narrow strip is cut from the rubber sheet

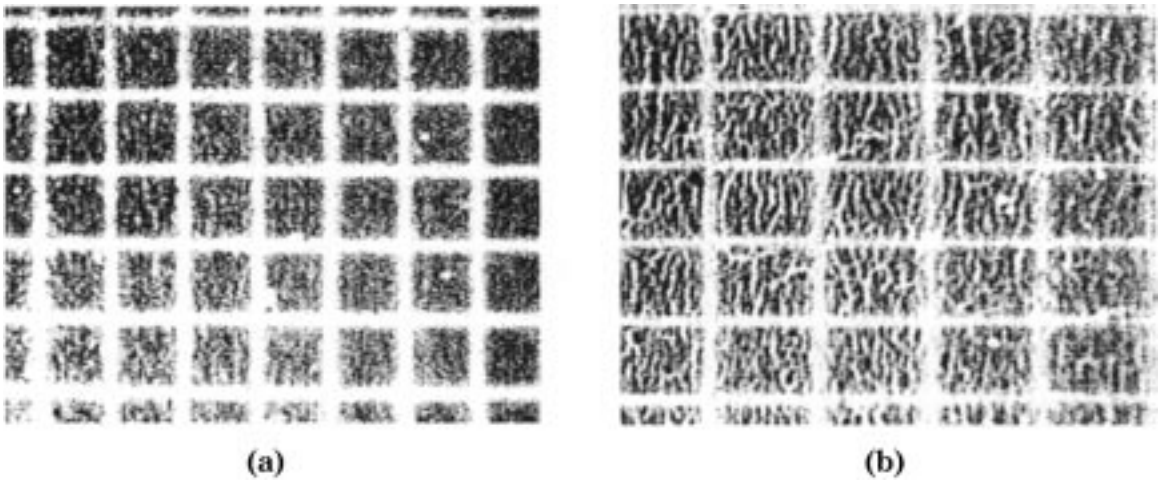

Figure 2. Optical micrograph of reference grid; (a) undeformed grid on natural rubber; (b) deformed grid on natural rubber (12.5×).

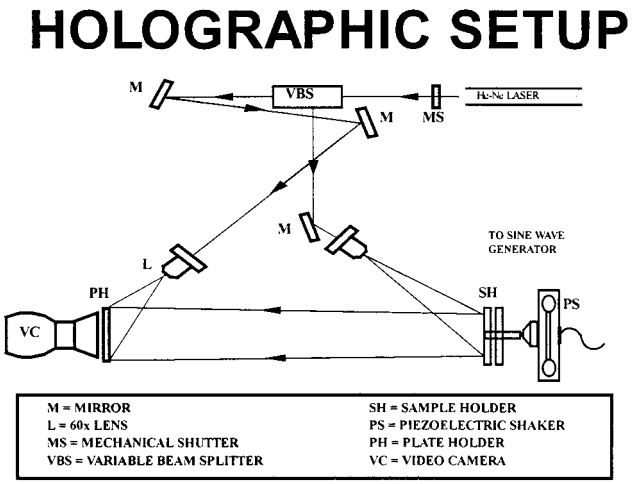

Figure 3. Illustration of real time holographic interferometry apparatus.

with the edges of the strip aligned along the edge of the superimposed mesh pattern and is clamped between two Invar washers that are designed to bolt together. The true stress of the strip is then measured, using holographic interferometry, as a function of temperature with the same sample being used at different extension ratios.

For the case of anisotropic biaxial extension, the film is stretched to different extension ratios in orthogonal directions to generate a state of anisotropic biaxial stress. An Invar washer is then bonded to the stretched film using an epoxy of Shell's EPON 828 (diglycidyl ether of Bisphenol A type epoxy resin) with a V-40 (a polyamino amide) curing agent to preserve the state of strain in the film. For both uniaxial and anisotropic biaxial extension, the strain is accurately determined by measuring the mesh deformation using an optical microscope. Figure 2 shows the grid pattern for a membrane before deformation and after stretching to a state of anisotropic biaxial extension deformation.

The holographic interferometer used in this work has been described previously, but a brief explanation of the apparatus will be given here.[44] Figure 3 depicts the holographic setup. During operation, a He−Ne laser beam is split into an objective and a reference beam by a beam splitter. The reference beam is reflected off a mirror through a diffuser to a thermoplastic photographic plate. The objective beam is reflected from a mirror, through a diffuser to the sample, and then reflected off the sample face to the thermoplastic plate. During the experiment, a static image of the sample is developed upon the thermoplastic plate. When the two wave fronts combine at the plate, an interference pattern depicting the virtual

Figure 4. Holographic pattern (1,1 mode) for a membrane in anisotropic biaxial extension at 367 Hz.

three-dimensional image of the sample in the object plane results. This pattern is observed using a video camera that looks through the thermoplastic plate.

During testing, the sample is rigidly fixed in a vacuum chamber with the potential for temperature control. This vessel is connected to a piezoelectric shaker or electromagnetic shaker that is driven by a sine wave generator. The resonant frequencies are determined by steadily increasing the frequency until the membrane resonates. The resonance is depicted by the appearance of the associated mode shape when observing the interference pattern on a TV monitor. Examples of these patterns for a rubber membrane under anisotropic biaxial stress with the corresponding mode numbers are depicted in Figures 4−8. After establishing the resonant frequencies, the corresponding stresses may be established from eq 30. Table 1 depicts typical data for a rubber membrane in a state of anisotropic biaxial extension. As the temperature of the vacuum chamber is changed, the stress of the membrane can be measured as a function of temperature.

Results and Discussion

Biaxial Data. Table 2 shows the numerical data taken from the thermoelastic measurements of pale

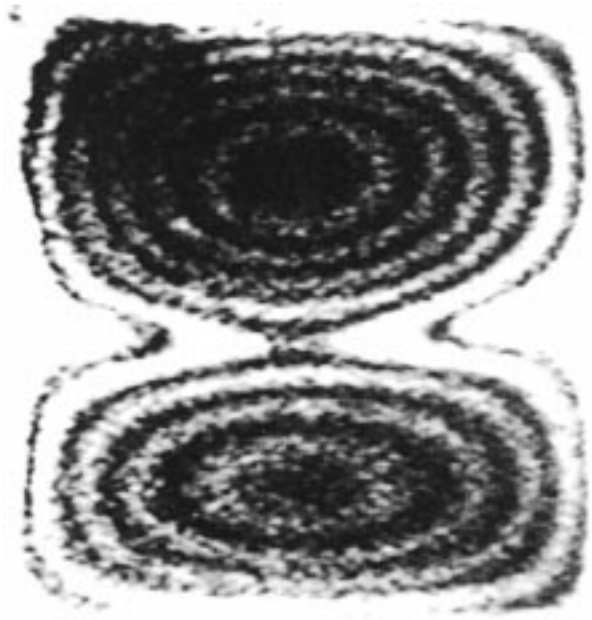

Figure 5. Holographic pattern (2,1 mode) for a membrane in anisotropic biaxial extension at 626 Hz.

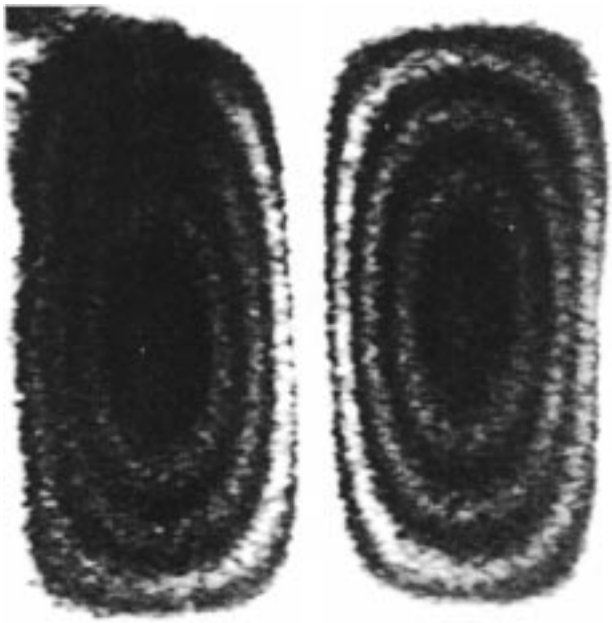

Figure 6. Holographic pattern (1,2 mode) for a membrane in anisotropic biaxial extension at 548 Hz.

crepe natural rubber in a state of anisotropic biaxial extension. In Appendix 2, constitutive equations are obtained from the strain energy function given in eq 31 for the case of anisotropic biaxial extension. The derivations result in eqs 60 and 61 and are shown below

$$\sigma'_1 J(T,T_o) = 2C_{100}(T,T_o)\left(\lambda_1^2(T_o) - \frac{J^2(T,T_o)}{\lambda_1^2(T_o)\,\lambda_2^2(T_o)}\right) \tag{39}$$

$$\sigma'_2 J(T,T_o) = 2C_{100}(T,T_o)\left(\lambda_2^2(T_o) - \frac{J^2(T,T_o)}{\lambda_1^2(T_o)\,\lambda_2^2(T_o)}\right) \tag{40}$$

where $\sigma'_1 = \sigma_1 - P$ and $\sigma'_2 = \sigma_2 - P$. The dilatational

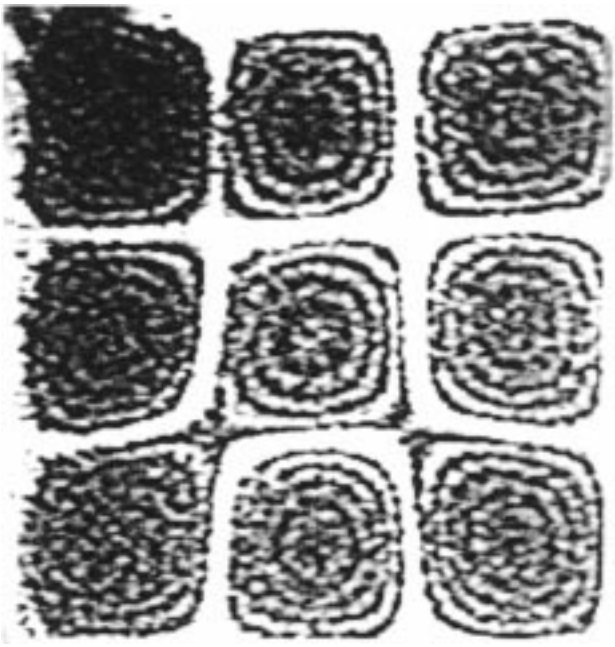

Figure 7. Holographic pattern (3,3 mode) for a membrane in anisotropic biaxial extension.

Figure 8. Holographic pattern (2,3 mode) for a membrane in anisotropic biaxial extension at 911 Hz.

term for these equations is given in eq 62 from Appendix 2 as

$$-P = 2C_{100}(T,T_o)J(T,T_o)\left(\frac{1}{\lambda_1^2(T_o)\,\lambda_2^2(T_o)} - e^{-4\alpha\Delta T}\right) + 4C_{002}(T,T_o)J^3(T,T_o) + 4C_{002}(T,T_o)J(T,T_o)e^{6\alpha\Delta T} \tag{41}$$

The roots of this relationship can be solved explicitly or determined by linearizing the relationship with respect to $J(T,T_o)$, resulting in eq 63 in Appendix 2. The experimental conditions require that measurements are taken under vacuum, which implies that the pressure term is equal to zero.

The values for the constants $C_{100}(T,T_o)$ and $C_{002}(T,T_o)$ are derived in Appendix 2 in terms of the linear elastic

Table 1. Holographic Data for a Typical Membrane in Anisotropic Biaxial Extension (λ_1(70 °C) = 1.21, λ_2(70 °C) = 1.08) Including the Frequency Calculated from Eq 30

ν_{mn} (Hz)	m	n	calcd freq (Hz)	$\sigma_1 J(T,70\ °C)$ (MPa)	$\sigma_2 J(T,70\ °C)$ (MPa)
367	1	1	374	0.210	0.137
548	1	2	553		
626	2	1	627		
749	2	2	748		
764	1	3	762		
901	3	1	904		
911	2	3	914		

Table 2. Thermoelastic Data of Natural Rubber in a State of Anisotropic Biaxial Extension

temp (K)	$\lambda_1(T_o)$	$\lambda_2(T_o)$	$\sigma_1 J(T,T_o)$ (MPa)	$\sigma_2 J(T,T_o)$ (MPa)
343	1.21	1.08	0.210	0.137
333	1.21	1.08	0.206	0.135
323	1.21	1.08	0.202	0.133
313	1.21	1.08	0.197	0.131
303	1.21	1.08	0.193	0.126
293	1.21	1.08	0.188	0.126
343	1.33	1.14	0.322	0.210
333	1.33	1.14	0.315	0.205
323	1.33	1.14	0.306	0.201
313	1.33	1.14	0.298	0.196
303	1.33	1.14	0.289	0.191
293	1.33	1.14	0.280	0.187
343	1.41	1.10	0.389	0.191
333	1.41	1.10	0.380	0.186
323	1.41	1.10	0.370	0.183
313	1.41	1.10	0.359	0.178
303	1.41	1.10	0.349	0.174
293	1.41	1.10	0.339	0.168
343	1.50	1.10	0.468	0.204
333	1.50	1.10	0.456	0.199
323	1.50	1.10	0.444	0.194
313	1.50	1.10	0.431	0.190
303	1.50	1.10	0.418	0.185
293	1.50	1.10	0.405	0.180
343	1.62	1.13	0.576	0.242
333	1.62	1.13	0.561	0.235
323	1.62	1.13	0.543	0.231
313	1.62	1.13	0.528	0.224
303	1.62	1.13	0.511	0.218
293	1.62	1.13	0.495	0.212

constants as eqs 69 and 72 and are shown below:

$$2C_{100}(T,T_o) = G(T,T_o)$$

$$C_{002}(T,T_o) = \frac{\kappa(T,T_o) + 2C_{100}(T,T_o)\left(\frac{1}{3} + e^{-4\alpha\Delta T}\right)}{4(3 - e^{6\alpha\Delta T})}$$

Using experimentally measured values of κ(298K,298K) = 2000 MPa, α = 220 ppm/°C, and C_{100}(298K,298K) = G(298K,298K)/2 = 0.108 MPa, eqs 39−41 allow the thermoelastic data to be modeled. Figures 9−13 display $\sigma_1 J(T,T_o)$, $\sigma_2 J(T,T_o)$, and $\Delta\sigma J(T,T_o)$ vs temperature along with the theoretical values. If $C_{100}(T,T_o) = C_{100}(T_o,T_o)$-$T/T_o$, where $C_{100}(T_o,T_o)$ is the Rivlin constant as a function of temperature, T_o, referenced to reference temperature, T_o, $C_{100}(T,T_o)$ can be determined from the slope of $\Delta\sigma J(T,T_o)$ vs temperature as shown by eq 35 and should intersect with the origin as the temperature approaches absolute zero. The energetic contribution to the rubber can be established using eq 36. Table 3 shows $\Delta\sigma J(T,T_o)$ vs temperature slopes, the intercept of the slope, and the relative energetic contribution to the stress. From Table 3, it can be seen that the calculated Rivlin constant, $C_{100}(T_o,T_o)$, compares favorably to the experimentally measured value of C_{100}(298K,298K) = 0.108 MPa and that the relative energetic contribution to the stress approaches zero.

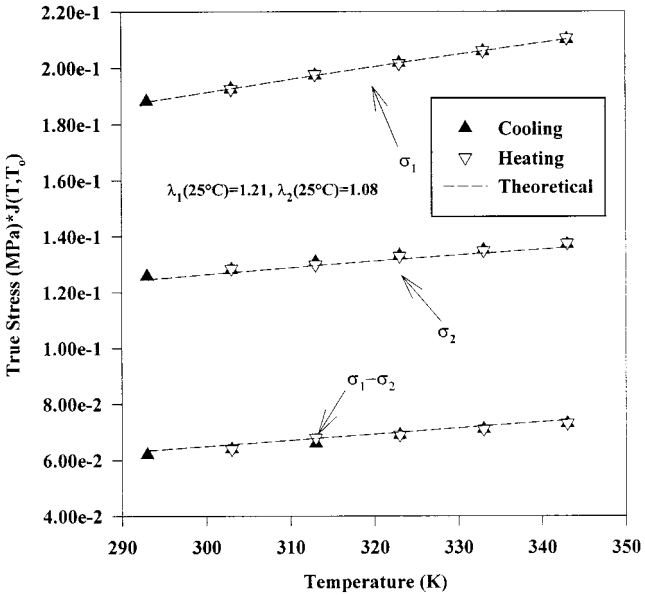

Figure 9. Plot of stress vs temperature for a rubber in anisotropic biaxial extension with λ_1(25 °C) = 1.21 and λ_2(25 °C) = 1.08. Theoretical fit is included in the figure.

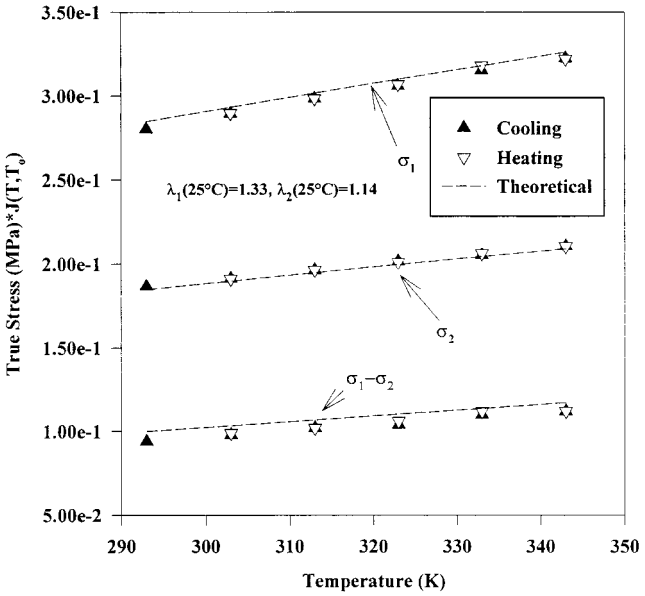

Figure 10. Plot of stress vs temperature for a rubber in anisotropic biaxial extension with λ_1(25 °C) = 1.33 and λ_2(25 °C) = 1.14. Theoretical fit is included in the figure.

Uniaxial Data. Table 4 shows the numerical data taken from the thermoelastic measurements of pale crepe natural rubber in a state of uniaxial extension. Using a derivation similar to that shown in Appendix 2, a uniaxial constitutive relationship can be derived from eq 31 as

$$\sigma_1 J(T,T_o) = 2C_{100}(T,T_o)\left(\lambda_1^2(T_o) - \frac{J(T,T_o)}{\lambda_1(T_o)}\right) \quad (42)$$

Likewise, the dilatational term can be evaluated in a manner similar to eq 63 in Appendix 2 for uniaxial

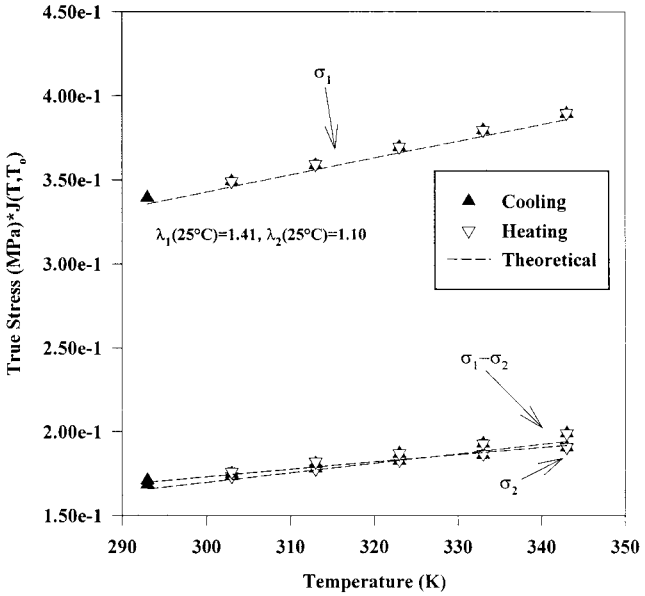

Figure 11. Plot of stress vs temperature for a rubber in anisotropic biaxial extension with $\lambda_1(25\ °C) = 1.41$ and $\lambda_2(25\ °C) = 1.10$. Theoretical fit is included in the figure.

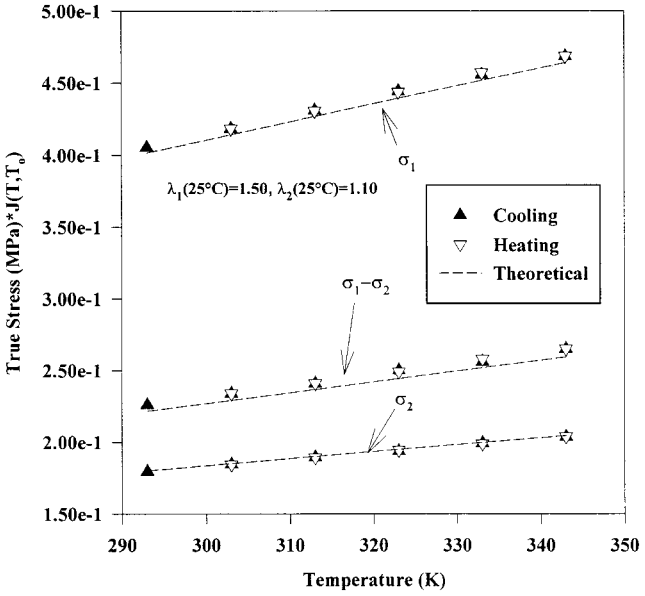

Figure 12. Plot of stress vs temperature for a rubber in anisotropic biaxial extension with $\lambda_1(25\ °C) = 1.50$ and $\lambda_2(25\ °C) = 1.10$. Theoretical fit is included in the figure.

conditions as

$$J(T,T_o) = \left[-P + 8C_{002}(T,T_o) - 2C_{100}(T,T_o)\frac{1}{\lambda_1(T_o)} + 8\alpha\Delta T(3C_{002}(T,T_o) - C_{100}(T,T_o))\right]/[-2C_{100}(T,T_o) + 8C_{002}(T,T_o)] \quad (43)$$

where P is the atmospheric pressure. Since the experimental measurements are taken under vacuum, the pressure term is set equal to zero. The material constants $C_{100}(T,T_o)$ and $C_{002}(T,T_o)$ have been previously defined. For this set of experiments, the following experimentally measured values were used in eq 42 to model the data in Table 4: κ(298K,298K) = 2000 MPa,

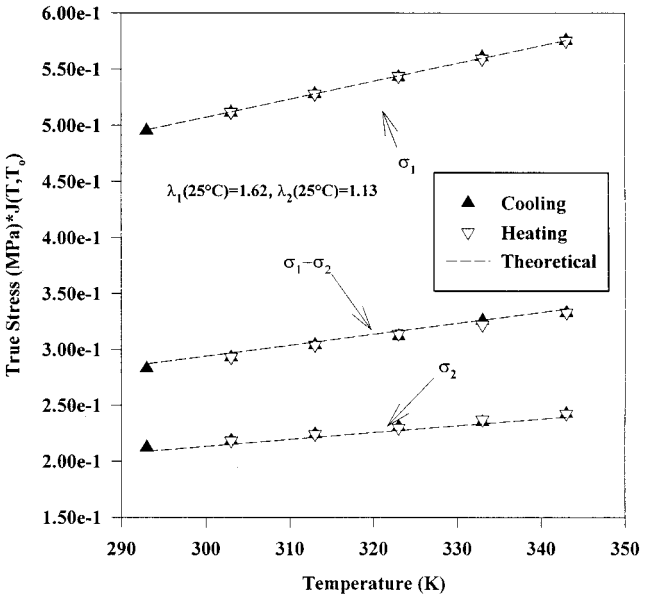

Figure 13. Plot of stress vs temperature for a rubber in anisotropic biaxial extension with $\lambda_1(25\ °C) = 1.62$ and $\lambda_2(25\ °C) = 1.13$. Theoretical fit is included in the figure.

α = 220 ppm/°C, and C_{100}(298K,298K) = G(298K, 298K)/2 = 0.126 MPa. The theoretical and experimental results are shown in Figure 14.

Existing thermoelastic data can also be modeled using eq 42. Shen and Blatz conducted uniaxial thermoelastic experiments under constant (atmospheric) pressure.[16] In modeling their data, the measured stress was assumed to be referenced to the current temperature, which in our notation is $\bar{\sigma}_1^o(T,T)$, and for this analysis Shen and Blatz's data was referenced to a fixed temperature, (i.e., $\sigma_1^o(T,T_o) = \bar{\sigma}_1^o(T,T)e^{2\alpha\Delta T}$). The expression shown in eq 42 is very similar to the result obtained from ideal rubber elasticity except that the material constants and extension ratios are referenced to a particular temperature. Also, the material is not assumed to be incompressible, and dilatation behaves according to eq 43. Table 5 shows dilatational values as a function of increasing extension ratio and temperature. It is noted that the dilatation is very close to unity for isothermal deformation, which is the assumption that the classical approach to thermoelasticity uses. However, when there is a change in temperature, the elastomeric material still has volumetric expansion in the unconstrained dimensions. This is shown in Table 5 where it is observed that the dilatation has a strong dependence upon the temperature.

Shen and Blatz reported the variables G(303K,303K) = 0.223MPa and $\alpha = 2.2 \times 10^{-4}$ K^{-1}, which were used in modeling the thermoelastic data. For the remaining variables, the pressure, P, was set equal to zero, and the bulk modulus was set equal to 2000 MPa for all temperature values. For our model, $G(T,T_o) = G(T_o,T_o)$-T/T_o with $G(T_o,T_o) = G$(303K,303K). The other material constant, $C_{002}(T,T_o)$, was evaluated by the use of eq 72 derived in Appendix 2 (e.g., C_{002}(303K,303K) = 83.4 MPa). Figure 15 shows the calculated results along with the experimental data generated by Shen and Blatz. Inspection of this figure indicates that a thermoelastic inversion point is accurately predicted by eq 42 and is a result of using a proper reference point. The statistical theory assigns all of the temperature dependence to the shear modulus (i.e., $G \sim T$) and fails to predict an

Table 3. Analysis of Anisotropic Biaxial Data

extension ratios	$(\partial\Delta\sigma J(T,T_o)/\partial T)_{J(T,T_o),\lambda_1(T_o),\lambda_2(T_o)}$	C_{100}(298K,298K) (MPa)	$\Delta\sigma_E/\Delta\sigma$
λ_1(298K) = 1.21	intercept = 1.17E−3	0.105	0.0057
λ_2(298K) = 1.08	slope = 2.100E−4		
λ_1(298K) = 1.33	intercept = −0.0108	0.114	0.113
λ_2(298K) = 1.14	slope = 3.600E−4		
λ_1(298K) = 1.41	intercept = 2.62E−3	0.109	0.011
λ_2(298K) = 1.10	slope = 5.714E−4		
λ_1(298K) = 1.50	intercept = 1.90E−5	0.110	0.002
λ_2(298K) = 1.10	slope = 7.710E−4		
λ_1(298K) = 1.62	intercept = −3.34E−3	0.108	−0.013
λ_2(298K) = 1.13	slope = 9.800-E−4		

Table 4. Thermoelastic Data of Natural Rubber in Uniaxial Extension

	$\sigma_1 J(T,T_o)$ (MPa)						
$\lambda_1(T_o)$	343 K	333 K	323 K	313 K	303 K	293 K	283 K
1.180	0.158	0.156	0.156	0.154	0.152	0.151	0.150[d]
1.210	0.174	0.172	0.169	0.165	0.163	0.160	0.156
1.260	0.210	0.208	0.206	0.204	0.200[a]	0.196[b]	0.193[d]
1.280	0.225	0.223	0.219	0.211	0.207	0.205[c]	0.201
1.640	0.558	0.549	0.539	0.525	0.512	0.501	0.490
1.780	0.726	0.717	0.703	0.689	0.673	0.655	0.647[d]
2.270	1.350	1.303	1.298	1.261	1.235	1.212	1.186

[a] Measurement temperature was 304 K. [b] Measurement temperature was 292 K. [c] Measurement temperature was 295 K. [d] Measurement temperature was 284 K.

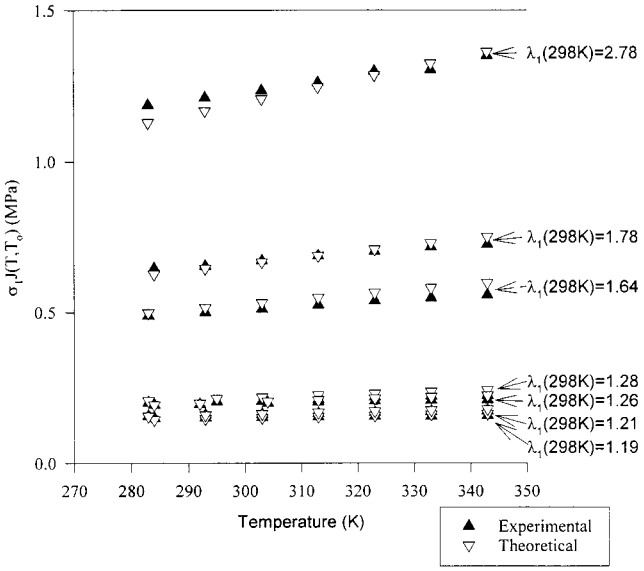

Figure 14. Plot of stress vs temperature for a natural rubber in uniaxial extension. A theoretical fit of the data is also plotted.

inversion point because all stress vs temperature slopes are positive.

Conclusion

When describing any thermomechanical deformation, it is best to consider the process in two parts. First, stress-free changes in dimensions resulting from thermal expansion need to be taken into account. Second, isothermal deformations resulting from an applied stress need to be assessed. Ignoring this two-step process is one of the shortcomings of many previous interpretations of thermoelastic theory. These interpretations lock parameters that depend on the initial configuration to a particular value (e.g., λ) and do not properly map the effect of temperature changes. A proper reference state for the moduli also needs to be established. Traditionally, the modulus of a rubber is

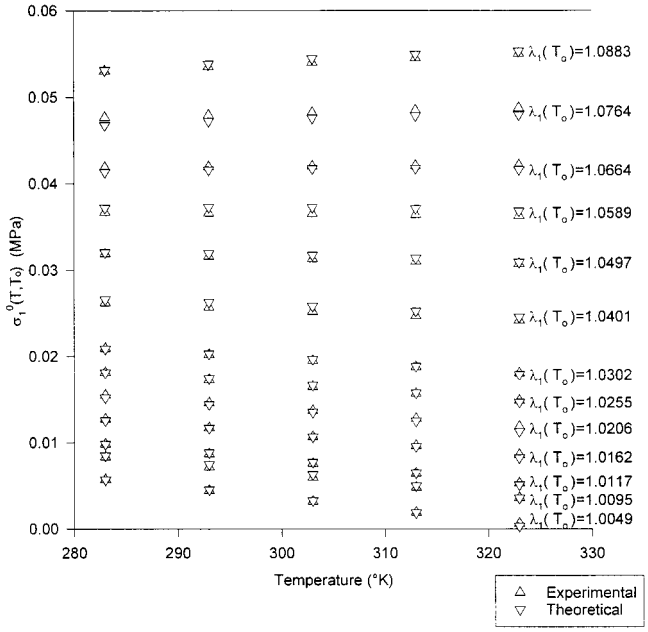

Figure 15. Stress-temperature data of Shen and Blatz for "infinitesimal" strain (butt-jointed sample[13]) along with the theoretical fit generated by eq 42.

assumed to be directly proportional to the absolute temperature, but it is not acknowledged that it has to be referenced to a temperature. For example, an ideal rubber has a modulus, $G(T,T_o) = N_o RT$, but this is only true if referenced to the reference temperature, T_o. If instead it is referenced to temperature, T, it is only entropic if $\bar{G}(T,T) = N_o RT e^{-\alpha(T-T_o)}$.

If the effect of thermal expansion is ignored, the thermodynamic analysis of rubber elasticity yields a nonzero term for the energetic contribution to the force. This result violates one of the basic assumptions of the theory in that the internal energy is independent of elongation. When the changes in dimensions resulting from thermal expansion are accounted for and if the material constants are referenced to a particular temperature, the energetic contribution is equal to zero.

When thermoelastic measurements are made, real time holographic interferometry has several advantages over traditional thermoelastic methods that make use of a load cell. Holographic interferometry directly measures the true stress of the membrane and has none of the electronic drifts associated with load cells. Also, problems associated with thermal expansion of the constraining hardware can be effectively neglected. The hardware used to constrain the membrane at fixed extension ratios does not change with temperature, because the constraining washer is made out of a material with a low coefficient of thermal expansion.

It is also possible to directly measure the true stresses of a thin film with this technique. More specifically, this

Table 5. Dilatational Values Calculated from Eq 43 for Different Temperatures and Extension Ratios

λ_1(303K)	$J(T$,283K)	$J(T$,293K)	$J(T$,303K)	$J(T$,313K)	$J(T$,323K)	$J(T$,333K)
1.00	0.9867	0.9933	0.9999	1.0066	1.0131	1.0197
1.05	0.9868	0.9934	0.9999	1.0065	1.0131	1.0197
1.10	0.9868	0.9934	1.0000	1.0066	1.0131	1.0197
1.30	0.9868	0.9934	1.0000	1.0066	1.0132	1.0198
1.50	0.9868	0.9934	1.0000	1.0066	1.0132	1.0198
2.00	0.9868	0.9934	1.0000	1.0066	1.0132	1.0198

technique allows resolution of the two principal stresses for a rubber film in a state of anisotropic biaxial stress. Subtracting the two principal stresses allows simplification of modeling from a phenomenological approach because symmetric terms of the strain density expansion drop out. Depending on the particular expansion of the strain density used, the remaining terms may be directly related to the entropic contribution to the force. From an experimental approach, measuring the two principal stresses is more advantageous than the uniaxial case because there is no difference between taking measurements at constant volume vs constant pressure for the biaxial case.

Appendix 1

The energetic contribution to the force is often derived by using the partial $(\partial f/\partial T)_{\bar{V}(T),\lambda_1(T_o)}$. However, it is experimentally difficult to constrain the sample at constant volume during deformation. Because most experiments are carried out under constant pressure, the partial is taken as the change in stress with temperature at constant pressure and constant $\lambda_i(T_o)$. We are interested in the same type of relationship based upon $\Delta\sigma = \sigma_1 - \sigma_2$ where σ_1 and σ_2 are the true principal stresses.

Starting with a strain energy function in terms of the extension ratios referenced to T_o

$$dW = [\sigma_1\, d(\ln(\lambda_1(T_o))) + \sigma_2\, d(\ln \lambda_2(T_o)) + \sigma_3\, d(\ln(\lambda_3(T_o)))]\bar{V}(T) \quad (44)$$

The true stress may be redefined for a state of anisotropic biaxial stress with imposed hydrostatic pressure, P:

$$\sigma_1 = \sigma'_1 - P, \quad \sigma_2 = \sigma'_2 - P, \quad \sigma_3 = -P$$

The strain density becomes upon rearrangement

$$dW = [\sigma'_1 J(T,T_o)\, d(\ln \lambda_1(T_o)) + \sigma'_2 J(T,T_o)\, d(\ln \lambda_2(T_o)) - P\, dJ(T,T_o)]V_o(T_o) \quad (45)$$

where $V_o(T_o)$ is the undeformed volume and $J(T,T_o)$ is the dilatation defined by $J(T,T_o) = \bar{V}(T)/V_o(T_o)$.

The stress vs temperature behavior of reversible deformations can be derived from the combined first and second laws of thermodynamics

$$dU = T\, dS + dW \quad (46)$$

where dU, dS, and dW are the incremental changes in internal energy, entropy, and strain density.

Substituting eq 45 into eq 46 and setting $\tilde{U} = U/V(T_o)$ and $\tilde{S} = S/V(T_o)$ yields

$$d\tilde{U} = T\, d\tilde{S} + \sigma'_1 J(T,T_o)\frac{d\lambda_1(T_o)}{\lambda_1(T_o)} + \sigma'_2 J(T,T_o)\frac{d\lambda_2(T_o)}{\lambda_2(T_o)} - P\, dJ(T,T_o) \quad (47)$$

It then follows that

$$\left(\frac{\partial\tilde{U}}{\partial\lambda_1(T_o)}\right)_{\lambda_2(T_o),T,J(T,T_o)} = T\left(\frac{\partial\tilde{S}}{\partial\lambda_1(T_o)}\right)_{\lambda_2(T_o),T,J(T,T_o)} + \frac{\sigma_1 J(T,T_o)}{\lambda_1(T_o)} \quad (48)$$

and likewise for $(\partial\tilde{U}/\partial\lambda_2(T_o))_{\lambda_1(T_o),T,J(T,T_o)}$.

The incremental change in the Helmholtz free energy, F, is given by

$$dF = -S\, dT + dW \quad (49)$$

which together with eq 45 and with $\tilde{F} = F/V(T_o)$ and $\tilde{S} = S/V(T_o)$ yields

$$d\tilde{F} = -\tilde{S}\, dT + J(T,T_o)\frac{d\lambda_1(T_o)}{\lambda_1(T_o)} + \sigma'_2 J(T,T_o)\frac{d\lambda_2(T_o)}{\lambda_2(T_o)} - P\, dJ(T,T_o) \quad (50)$$

From above, it follows that

$$-\left(\frac{\partial\tilde{S}}{\partial\lambda_1(T_o)}\right)_{\lambda_2(T_o),T,J(T,T_o)} = \left(\frac{\partial(\sigma'_1 J(T,T_o)/\lambda_1(T_o))}{\partial T}\right)_{\lambda_1(T_o),\lambda_2(T_o),J(T,T_o)} \quad (51)$$

and likewise for $-(\partial\tilde{S}/\partial\lambda_2(T_o))_{\lambda_1(T_o),T,J(T,T_o)}$.

Substituting eq 51 into eq 48 yields

$$\left(\frac{\partial\bar{U}}{\partial(\ln(\lambda_1(T_o)))}\right)_{J(T,T_o),\lambda_2(T_o),T} = -T\left(\frac{\partial(\sigma'_1 J(T,T_o))}{\partial T}\right)_{J(T,T_o),\lambda_1(T_o),\lambda_2(T_o)} + \sigma'_1 J(T,T_o) \quad (52)$$

with a similar expression for $(\partial\bar{U}/\partial(\ln(\lambda_2(T_o))))_{J(T,T_o),\lambda_1(T_o),T}$.

Using

$$\left(\frac{\partial\sigma'_1 J(T,T_o)}{\partial T}\right)_{J(T_o),\lambda_1(T_o),\lambda_2(T_o)} = \left(\frac{\partial\sigma'_1 J(T,T_o)}{\partial T}\right)_{P,\lambda_2(T_o),\lambda_2(T_o)} + \left(\frac{\partial\sigma'_1 J(T,T_o)}{\partial P}\right)_{T,\lambda_1(T_o),\lambda_2(T_o)}\left(\frac{\partial P}{\partial T}\right)_{J(T,T_o),\lambda_1(T_o),\lambda_2(T_o)}$$

$$\left(\frac{\partial\bar{U}}{\partial(\ln(\lambda_1(T_o)))}\right)_{J(T,T_o),\lambda_2(T_o),T} = \sigma'_1 J(T,T_o) - T\left[\left(\frac{\partial\sigma'_1 J(T,T_o)}{\partial T}\right)_{P,\lambda_1(T_o),\lambda_2(T_o)} + \left(\frac{\partial\sigma'_1 J(T,T_o)}{\partial P}\right)_{T,\lambda_1(T_o),\lambda_2(T_o)}\left(\frac{\partial P}{\partial T}\right)_{J(T,T_o),\lambda_1(T_o),\lambda_2(T_o)}\right] \quad (53)$$

with a similar expression for $(\partial\tilde{U}/\partial(\ln(\lambda_2(T_o))))_{J(T,T_o),\lambda_1(T_o),T}$. The energetic contribution to the stress may be defined as

$$\left(\frac{\partial \tilde{U}}{\partial(\ln(\lambda_1(T_o))}\right)_{J(T,T_o),\lambda_2(T_o),T} = \sigma'_{1E} J(T,T_o)$$

with an equivalent expression for $(\partial\tilde{U}/\partial(\ln(\lambda_2(T_o))))_{J(T,T_o),\lambda_2(T_o),T}$.

Substituting this expression into eq 53 and subtracting the equivalent expression based upon $\lambda_2(T_o)$, σ'_2, and σ'_{2E} yields

$$\frac{\Delta\sigma'_E}{\Delta\sigma'} = 1 - T\frac{1}{\Delta\sigma' J(T,T_o)}\left[\left(\frac{\partial \Delta\sigma' J(T,T_o)}{\partial T}\right)_{P,\lambda_1(T_o),\lambda_2(T_o)} + \left(\frac{\partial P}{\partial T}\right)_{J(T,T_o),\lambda_1(T_o),\lambda_2(T_o)}\left(\frac{\partial \Delta\sigma' J(T,T_o)}{\partial P}\right)_{T,\lambda_1(T_o),\lambda_2(T_o)}\right] \quad (54)$$

where $\Delta\sigma'_E = \sigma'_{1E} - \sigma'_{2E}$ and $\Delta\sigma' = \sigma'_1 - \sigma'_2$.

Appendix 2

Equation 31 gives a possible strain energy function that reduces to linear thermoelasticity in the limit of small strains and finite temperature changes. The true stresses can be derived from the strain energy function using

$$\sigma_i V_o(T_o) = \frac{\lambda_i(T_o)}{J(T,T_o)}\left(\frac{\partial W(T,T_o)}{\partial \lambda_i(T_o)}\right)$$

The resulting stresses become

$$\sigma_i = 2C_{100}(T,T_o)\frac{\lambda_i^2(T_o)}{J(T,T_o)} + 2C_{001}(T,T_o)J(T,T_o) + 4C_{002}(T,T_o)J(T,T_o)(J^2(T,T_o) - e^{6\alpha\Delta T}) \quad (55)$$

The stresses must be equal to zero when the extension ratios referenced to temperature, T, are equal to one (i.e., $\bar{J}(T,T) = 1$, $\bar{\lambda}_1(T) = 1$). This requires $\lambda_1(T_o) = e^{\alpha\Delta T}$ and $J(T,T_o) = e^{3\alpha\Delta T}$ with the result $-C_{100}(T,T_o)e^{-4\alpha\Delta T} = C_{001}(T,T_o)$. The principal stresses become

$$\sigma_i = 2C_{100}(T,T_o)\left(\frac{\lambda_i^2(T_o)}{J(T,T_o)} - J(T,T_o)e^{-4\alpha\Delta T}\right) + 4C_{002}(T,T_o)J(T,T_o)(J^2(T,T_o) - e^{6\alpha\Delta T}) \quad (56)$$

To account for changes in pressure, σ_3, can be set equal to an imposed hydrostatic pressure, $-P$. A new series of principal true stresses can be defined to account for this applied pressure

$$\sigma'_1 = \sigma_1 - \sigma_3 \quad (57)$$

$$\sigma'_2 = \sigma_2 - \sigma_3 \quad (58)$$

$$\sigma_3 = -P \quad (59)$$

Assuming a state of anisotropic biaxial extension and using the definition of the dilatation, $J(T,T_o) = \lambda_1(T_o)\lambda_2(T_o)\lambda_3(T_o)$, one may write the principal stresses as

$$\sigma'_1 = 2C_{100}(T,T_o)\left(\frac{\lambda_1^2(T_o)}{J(T,T_o)} - \frac{J(T,T_o)}{\lambda_1^2(T_o)\lambda_2^2(T_o)}\right) \quad (60)$$

$$\sigma'_2 = 2C_{100}(T,T_o)\left(\frac{\lambda_2^2(T_o)}{J(T,T_o)} - \frac{J(T,T_o)}{\lambda_1^2(T_o)\lambda_2^2(T_o)}\right) \quad (61)$$

$$-P = 2C_{100}(T,T_o)J(T,T_o)\left(\frac{1}{\lambda_1^2(T_o)\lambda_2^2(T_o)} - e^{-4\alpha\Delta T}\right) + 4C_{002}(T,T_o)J^3(T,T_o) + 4C_{002}(T,T_o)J(T,T_o)e^{6\alpha\Delta T} \quad (62)$$

The dilatation can be solved from this last expression by solving the roots of the equation and linearizing the relationship with respect to $J(T,T_o)$ yielding

$$J(T,T_o) = [-P + 8C_{002}(T,T_o)]/\left[2C_{100}(T,T_o)\left(\frac{1}{\lambda_1^2(T_o)\lambda_2^2(T_o)} - e^{-4\alpha\Delta T}\right) + 4C_{002}(T,T_o)(3 - e^{6\alpha\Delta T})\right] \quad (63)$$

Evaluation of Material Constants. The constant $C_{100}(T,T_o)$ may be evaluated in terms of the linear thermoelastic constants for uniaxial deformation using eq 31 and $\sigma_1^o(T,T_o) = \partial W(T,T_o)/\partial(\lambda_1(T_o))$. Taking the partial of the calculated $\sigma_1^o(T,T_o)$ with respect to $\lambda_1(T_o)$ yields

$$\left(\frac{\partial \Delta\sigma^o(T,T_o)}{\partial(\lambda_1(T_o))}\right)_{P,T} = 2C_{100}(T,T_o)\left[1 - \frac{1}{\lambda_1^2(T_o)}\left(\frac{\partial(J(T,T_o))}{\partial(\lambda_1(T_o))}\right)_{P,T} + \frac{2J(T,T_o)}{\lambda_1^3(T_o)}\right] \quad (64)$$

The partial $(\partial(J(T,T_o))/\partial(\lambda_1(T_o)))_{P,T}$ can be evaluated by relating it to the equations of linear thermoelasticity. Assuming isothermal conditions and small strains, the dilatation as a function of temperature referenced to temperature, T_o, can be written as

$$J(T,T_o) = \frac{\bar{V}(T)}{V_o(T_o)} \cong \frac{1}{E(T,T_o)}(1 - 2\upsilon(T,T_o))(\sigma_{11}^o(T,T_o) + \sigma_{22}^o(T,T_o) + \sigma_{33}^o(T,T_o)) + 1 \quad (65)$$

where $\epsilon_{11}(T_o)$, $\epsilon_{22}(T_o)$, and $\epsilon_{33}(T_o)$ are the strains, $E(T,T_o)$ is Young's modulus, and $\upsilon(T,T_o)$ is Poisson's ratio. Setting $\sigma_{11}^o(T,T_o) = \hat{\sigma}_{11}^o(T,T_o) - P$, $\sigma_{22}^o(T,T_o) = -P$, and $\sigma_{33}^o(T,T_o) = -P$ and making use of Hooke's law (i.e., $\sigma_{ii}^o(T,T_o) = E(T,T_o)\epsilon_{ii}(T_o)$) and $\hat{\epsilon}_{11}(T_o) = \lambda_1(T_o) - 1$ yields

$$\left(\frac{\partial(J(T,T_o))}{\partial(\lambda_1(T_o))}\right)_{P,T} \cong 1 - 2\upsilon(T,T_o) \quad (66)$$

When $J(T,T_o)$ and $\lambda_1(T_o) = 1$, eq 64 becomes

$$\left(\frac{\partial(\Delta\sigma^o(T,T_o))}{\partial(\lambda_1(T_o))}\right)_{P,T} \cong 4C_{100}(T,T_o)(1 + \upsilon(T,T_o)) \quad (67)$$

The linear thermoelastic equivalent of eq 67 is

$$\left(\frac{\partial(\sigma_1^o(T,T_o))}{\partial(\lambda_1(T_o))}\right)_{P,T} = E(T,T_o) = 2G(T,T_o)(1+\upsilon(T,T_o)) \tag{68}$$

which necessarily implies

$$2C_{100}(T,T_o) = G(T,T_o) \tag{69}$$

To evaluate the material constant, $C_{002}(T,T_o)$, it is assumed there is an imposed hydrostatic pressure with no distortional component. In this case, $\sigma_1 = \sigma_2 = \sigma_3 = -P/3$ and $\lambda_1(T_o) = \lambda_2(T_o) = \lambda_3(T_o) = J^{1/3}(T,T_o)$, and the governing constitutive equation becomes

$$\frac{-P}{3} = [2C_{100}(T,T_o)J^{-1/3}(T,T_o) + 2C_{001}(T,T_o)J(T,T_o) + 4C_{002}(T,T_o)J(T,T_o)(J^2(T,T_o) - e^{6\alpha\Delta T})] \tag{70}$$

After the equation above is linearized with respect to the dilatation, the calculated bulk modulus is

$$\kappa(T,T_o) = -\left(\frac{\partial P}{\partial(J(T,T_o))}\right)_T = 3\left[2C_{100}(T,T_o)\left(-\frac{1}{3}\right) + 2C_{001}(T,T_o) + 4C_{002}(T,T_o)(3 - e^{6\alpha\Delta T})\right] \tag{71}$$

Previously, it was shown that $-C_{100}(T,T_o)e^{-4\alpha\Delta T} = C_{001}(T,T_o)$. Equation 71 upon rearrangement becomes

$$C_{002}(T,T_o) = \frac{\kappa(T,T_o)/3 + 2C_{100}(T,T_o)(^1/_3 + e^{-4\alpha\Delta T})}{4(3 - e^{6\alpha\Delta T})} \tag{72}$$

References and Notes

(1) Rivlin, R. S. *Philos. Trans. R. Soc. London, A* **1948,** *241*, 379.
(2) Flory, P. J.; Rehner, J. *J. Chem. Phys.* **1943**, *11*, 512.
(3) Lu, S. C. H.; Pister, K. S. *J. Solids Struct.* **1975**, *11*, 927.
(4) Lion, A. *J. Mech. Phys. Solids* **1997**, *45*, 1805.
(5) Humphrey, J. D.; Rajagopal, K. R. *J. Elasticity* **1998**, *49*, 189.
(6) Shen, M. *J. Appl. Phys.* **1970**, *41*, 4351.
(7) Hwo, C. H.; Bell, J. P.; Johnson, J. F. *J. Appl. Polym. Sci.* **1974**, *18*, 2865.
(8) Price, C. *Proc. R. Soc. London, A* **1976**, *351*, 331.
(9) Shen, M.; McQuarrie, D. A.; Jackson, J. L. *J. Appl. Phys.* **1967**, *38*, 791.
(10) Shen, M. *Macromolecules* **1969**, *2*, 358.
(11) Godovsky, Y. K. *Polymer* **1981**, *22*, 75.
(12) Shen. M.; Cirlin, E. H.; Gebhard, H. M. *Macromolecules* **1969**, *2*, 683.
(13) Chen, T. Y.; Ricica, P.; Shen, M. *J. Macromol. Sci.—Chem. A* **1973**, *7*, 889.
(14) Cirlin, E. H.; Gebhard, H. M.; Shen, M. *J. Macromol. Sci.—Chem. A* **1971**, *5*, 981.
(15) Shen, M.; Tobolsky, A. V. *J. Appl. Phys.* **1966**, *37*, 1952.
(16) Shen, M.; Blatz, P. J. *J. Appl. Phys.* **1968**, *39*, 4937.
(17) Vasko, M.; Bleha, T.; Romanov, A. *J. Macromol. Sci.—Rev Macromol. Chem. C* **1976**, *15*, 1.
(18) Wen, J.; Mark, J. E. *Polym. J.* **1994**, *26*, 151.
(19) Mark, J. E. *J. Polym. Sci., Macro. Macromol. Rev.* **1976**, *11*, 135.
(20) Mark, J. E. *Rubber Chem. Technol.* **1973**, *46*, 593.
(21) Mohsin, M. A.; Berry, J. P.; Treloar, L. R. G. *Br. Polym. J.* **1986**, *18*, 145.
(22) Fung, Y. C. *Foundations of Solid Mechanics;* Prentice Hall: Englewood Cliffs, NJ, 1965.
(23) Malvern, L. E. *Introduction to the Mechanics of a Continuous Medium*; Prentice Hall: Englewood Cliffs, NJ, 1969.
(24) Kawabata, S.; Kawai, H. *Advances in Polymer Science*; Springer-Verlag: Berlin, 1977; Vol. 24
(25) Matsuda, M.; Kawabata, S.; Kawai, H. *Macromolecules* **1981**, *14*, 1688.
(26) Blatz, P. J. *Polymer Networks: Structural and Mechanical Properties*; Plenum Press: New York, 1971.
(27) Treloar, L. R. G. *Trans. Faraday Soc.* **1943**, *39*, 36.
(28) Mooney, M. *J. Appl. Phys.* **1940**, *11*, 582.
(29) Blatz, P. J. *Rubber Chem. Technol.* **1963**, *36*, 1459.
(30) Macknight, W. J.; Aklonis, J. J. *Introduction to Polymer Viscoelasticity*; John Wiley & Sons: New York, 1983.
(31) Lyon, R. E.; Farris, R. J. *Polymer* **1987**, *28*, 1127.
(32) Kawabata, S.; Matsuda, M.; Tei, K.; Kawai, H. *Macromolecules* **1981,** *14*, 155.
(33) Obata, Y.; Kawabata, S.; Kawai, H. *J. Polym. Sci., Part A-2* **1970,** *8*, 903.
(34) Stein, R. S. *SPE Trans.* **1961**, *1*, 164.
(35) Xu, P.; Mark J. E. *J Polym. Phys.* **1991**, *29*, 355.
(36) Jou, C.; Farris, R. J. *Exp. Mech.* **1994**, *34*, 306.
(37) Maden, M. A.; Jagota, A.; Mazur, S.; Farris, R. J. *J. Am. Ceram. Soc.* **1994,** *77*, 625.
(38) Tong, Q. K.; Maden, M. A.; Jagota, A.; Farris, R. J. *J. Am. Ceram. Soc.* **1994**, *77*, 638.
(39) Vrtis, J. K.; Farris, R. J. *J. Appl. Polym. Sci.* **1996**, *59*, 440.
(40) Vrtis, J. K.; Farris, R. J. *Proc. Am. Chem. Soc., Div. Polym. Mater. Sci. Eng.* **1993,** *69*, 440.
(41) Pines, B. Y.; Andronov, V. M.; Rabukhin, V. B. *Ind. Lab.* **1968**, *35*, 887.
(42) Leissa, A. W. *Vibration of Plates*; NASA SP-160; National Aeronautics and Space Administration: Washington, DC, 1969.
(43) Tong, Q. K. Ph.D. Dissertation, University of Massachusetts, Amherst, MA, 1993.
(44) Maden, M. A. Ph.D. Dissertation, University of Massachusetts, Amherst, MA, 1992.

MA9806763